Electronic Supplementary Material (ESI) for Journal of Materials Chemistry A.
This journal is © The Royal Society of Chemistry 2020

Supplementary Information

Assembling of Polymer and Metal Nanoparticle Coated Glass Capillary Array for Efficient Solar Desalination

*Yukang Fan[a], Shuo Wang[a], Fei Wang[a], Jingxian He[a], Zhuoyue Tian[a], Huyang Zhao[a], Zhaoqi Zhu[a], Hanxue Sun[a], Weidong Liang[a], An Li[a]**

[a] College of Petrochemical Technology, Lanzhou University of Technology, Langongping Road 287, Lanzhou 730050, P. R. China

*Corresponding author. Tel: +86-931-2973305. Fax: +86-931-2973305. E-mail address: lian2010@lut.cn (An Li).

1. Characterization

The morphology of the PDA-GCA and PDN-GCA were taken on scanning electron microscope (TESCAN MIRA3) equipped with an energy dispersive spectroscopy (EDS) under a vacuum environment at 15 kV. XPS spectra were obtained using a Physical Electronics 5000 Versa Probe II Scanning ESCA (XPS) Microprobe. The optical absorption properties of the polydopamine particles and palladium nanoparticles were measured by UV-vis-NIR spectrometer from 200~2500 nm equipped with an integrating sphere to collect the scattered light for accurate measurement (PerkinElmer Lambda 750). Flourier transform infrared spectroscopy (FTIR) was recorded from in the range of 4000-400 cm^{-1} by using a Mexus 670 spectral instrument. The thermal conductivity of multilayer cotton fibers was investigated on flash method thermal analyzer (DRE-III, China). The contact angle images of the GCA, PDA-GCA and PDN-GCA were measured using a contact angle apparatus (SL200KB).

2. Solar steam generation testing.

The solar steam generation experiments was conducted at a lab-made, online, real-time measurement system for 60 minutes which is consisted of (a) a solar light simulator (xenon arc lamp, CEL-S500, Ceaulight), (b) a solar filter (AM 1.5, Ceaulight), (c) an analytical balance with a maximum measuring range of 200 g (FA 2004), (d) a computer to record the real-time mass reduction for steam generation, (e) an infrared (IR) camera to record the surface temperature of samples (Testo 869, Germany). Measured light intensity by a full spectrum optical power meter (CEL-NP2000-2, Beijing Education Au-light Co., Ltd.). The samples were placed on the wood residue and sea sand containing water, the

multilayer cotton fibers on the bottom of glass capillary. The relative position of the multi-layer cotton fibers and water surface is on the water surface, the bottom contact with the water, the upper contact with GCA-based evaporator. The room temperature was maintained at 18~24 ^{o}C and it ranged the humidity from 45% to 55% during every test.

Salt-resistance experiment

The salt-resistance experiment for the PDN-GCA was performed with the Dalian sea water (K^{+} 419.3 mg L^{-1}, Ca^{2+} 396.4 mg L^{-1}, N^{a+} 7407 mg L^{-1}, Mg^{2+} 1081 mg L^{-1}) and NaCl solution (the concentration of 3.5 wt.%, 5 wt.%, 10 wt.%, 15 wt.%, 20 wt.%).

3. Calculation of the energy conversion efficiency

$$\eta = m\, h_{Lv} / C_{opt}\, q_i$$

where m is the mass flux of steam (the rate of water evaporation under the dark condition subtracted), C_{opt} is the optical concentration, q_i is the nominal direct solar irradiation 1 kW m^{-2}, h_{Lv} denotes total enthalpy of liquid-vapor phase change (including sensible heat and phase-change enthalpy), can be calculated as:

$$h_{Lv} = \lambda + C\Delta T$$

where λ is latent heat of phase change (2256 kJ kg^{-1}), C is specific heat capacity of water (4.2 kJ kg^{-1} K^{-1}), and ΔT denotes the temperature increment of the water.

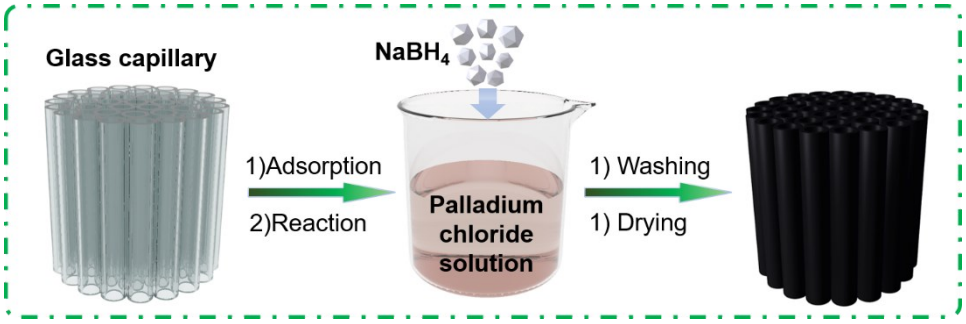

Figure S1. The fabrication diagram of PDN-GCA.

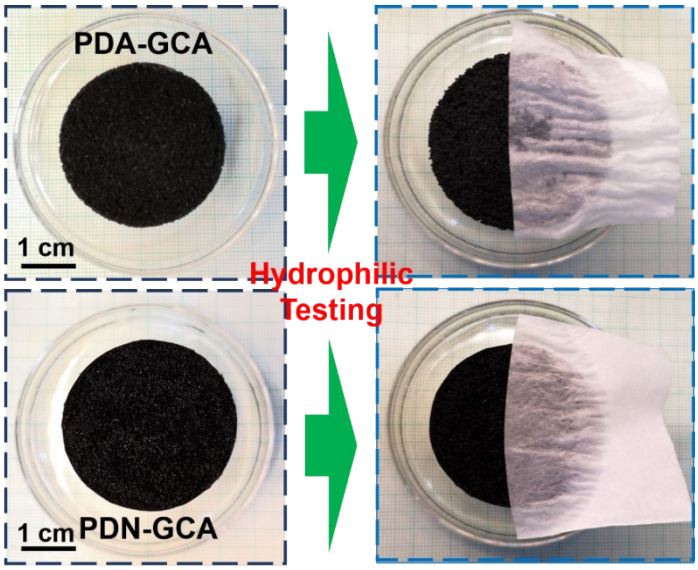

Figure S2. Water transportation performance testing of PDA-GCA and PDN-GCA.

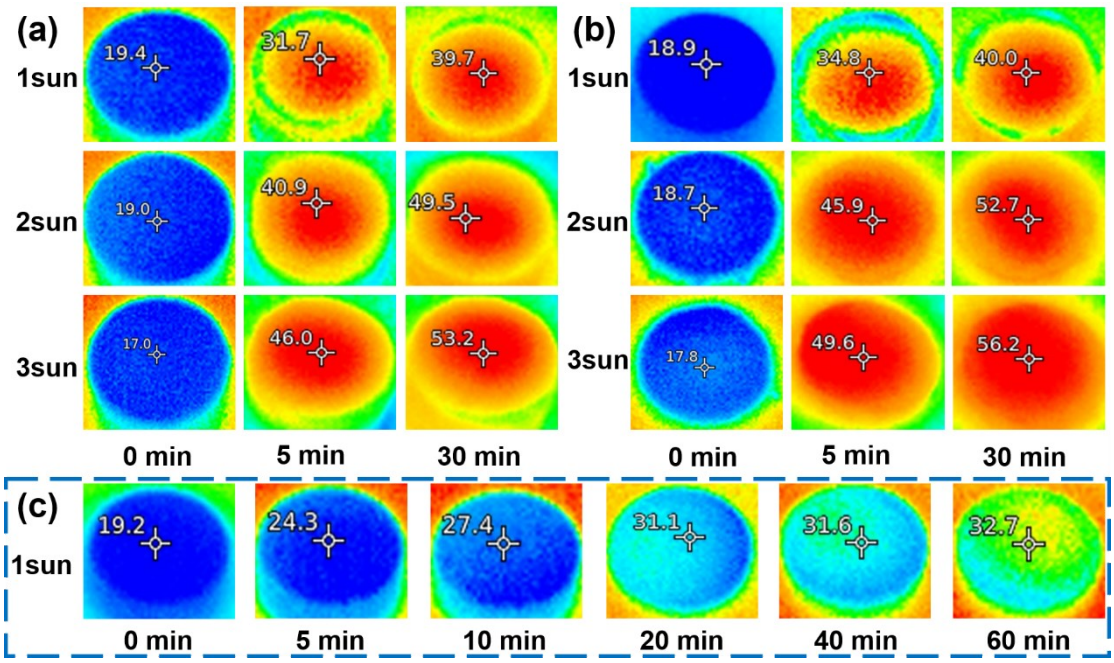

Figure S3. (a) Top-view infrared (IR) images of PDA-GCA under different illuminations for different times. (b) Top-view infrared (IR) images of PDN-GCA under different illuminations for different times. (c) Top-view infrared (IR) images of blank GCA under 1 kW·m^{-2} illumination for different times.

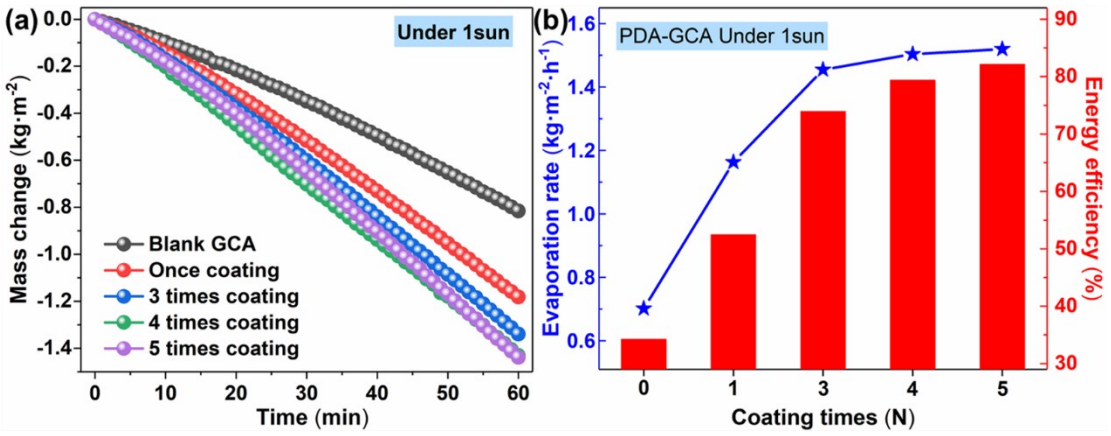

Figure S4. (a) Time-dependent mass change curves of water with different coating times for PDA-GCA under 1kW m^{-2} illumination. (b) The evaporation rate and energy conversion efficiency of PDA-GCA with different coating times under 1kW m^{-2} illumination.

The photothermal evaporation efficiency of PDA-GCA for different deposition times were investigated. As shown in Figure S4a, b, it is clear that the difference of evaporation rate between GCA coated for the first time and GCA not coated is large, and that GCA coated three times has a higher evaporation rate than GCA coated once, and almost the same as GCA coated five times.

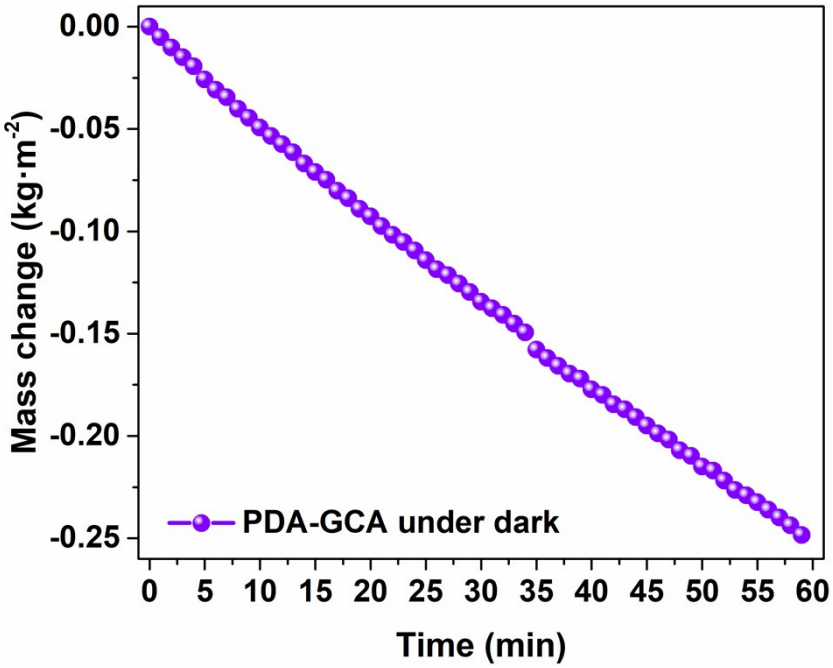

Figure S5. Time-dependent mass change curves of water for PDA-GCA under dark condition.

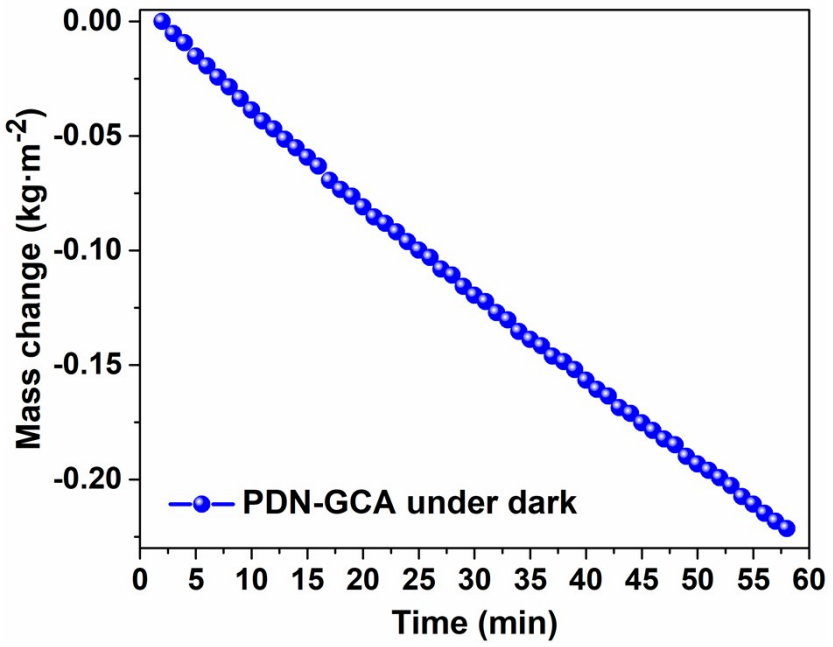

Figure S6. Time-dependent mass change curves of water for PDN-GCA under dark condition.

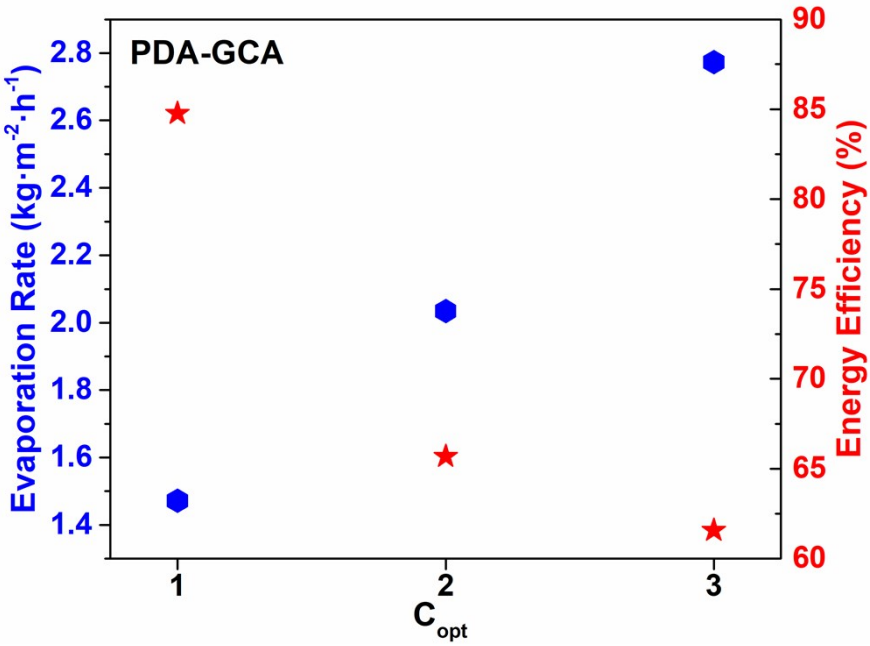

Figure S7. The evaporation rate and energy conversion efficiency of PDA-GCA solar desalination with water under 1, 2 and 3 kW·m^{-2} illumination.

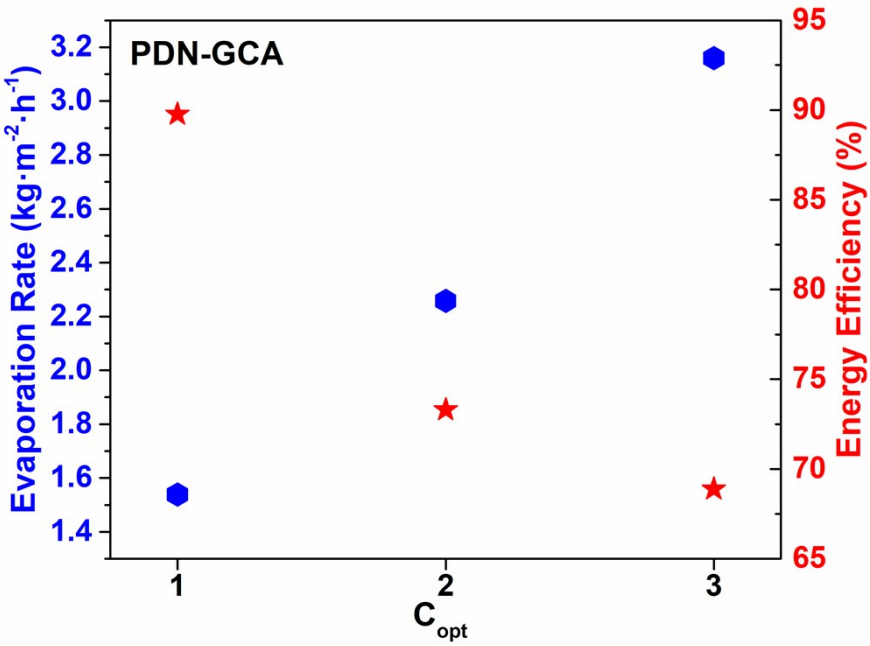

Figure S8. The evaporation rate and energy conversion efficiency of PDN-GCA solar desalination with water under 1, 2 and 3 kW·m^{-2} illumination.

Table S1. The comparison of steam generation performance of this work and the previously reported under different irradiation

Reference	Materials	Solar irradiation	Evaporation efficiency
1	AuNPs[1]	1 kW·m^{-2}	63.1%
2	Bi_2Se_3 nanosheets[2]	1 kW·m^{-2}	68%
3	Plasmonic wood[3]	1, 10 kW·m^{-2}	68.5%, 85%
4	Plasmonic biofoam[4]	5.1 kW·m^{-2}	76.3%
5	PDA/BNC bilayer foams[5]	1 kW·m^{-2}	78%
6	PPy-coated membranes[6]	1 kW·m^{-2}	81.9%
7	MoS_2 nanosheets[7]	5.35 kW·m^{-2}	82%
8	CNF@RGO-*n*[8]	1 kW·m^{-2}	83%
9	rGO/nickel foam[9]	1 kW·m^{-2}	83.4%
10	MXene[10]	1 kW·m^{-2}	84%
11	PDA-coated wood[11]	1 kW·m^{-2}	87%
This work	PDA-GCA	1 kW·m^{-2}	85.8%
This work	PDN-GCA	1 kW·m^{-2}	89.8%

References:

1 T. Li, Q. Fang, H. Lin and F. Liu, *J. Mater. Chem.*, 2019, **7**, 17505-17515.

2 Y. Liu, Y. Zhang and G. Jia, *Energy Reports*, 2020, **206**, 110347.

3 M. Zhu, Y. Li, F. Chen, X. Zhu, J. Dai, Y. Li, Z. Yang, X. Yan, J. Song and Y. Wang, *Adv. Energy Mater.*, 2018, **8**, 1701028.

4 L. Tian, J. Luan, K. K. Liu, Q. Jiang, S. Tadepalli, M. K. Gupta, R. R. Naik and S. Singamaneni, *Nano Lett.*, 2015, **16**, 609-616..

5 Q. Jiang, H. G. Derami, D. Ghim, S. Cao, Y. S. Jun and S. Singamaneni, *J. Mater. Chem. A*, 2017, **5**, 18397-18402.

6 C. Wang, Y. Wang, X. Song, M. Huang and H. Jiang, *Adv. Sustain. Syst.*, 2019, **3**, 1800108.

7 D. Ghim, Q. Jiang, S. S. Cao, S. Singamaneni and Y. S. Jun, *Nano Energy*, 2018, **53**, 949-957.

8 W. Wei, Q. Guan, C. You, J. Yu, Z. Yuan, P. Qiang, C. Zhou, Y. Ren, Z. You and F. Zhang, *J. Mater. Chem. A*, 2020, **8**, 13927-13934.

9 X. Shan, Y. Lin, A. Zhao, Y. Di and Z. Gan, *Nanotechnology*, 2019, **30**, 425403.

10 R. Li, L. Zhang, L. Shi and P. Wang, *ACS nano*, 2017, **11**, 3752-3759.

11 X. Wu, G. Y. Chen, W. Zhang, X. Liu and H. Xu, *Adv. Sustain. Syst.*, 2017, **1**, 1700046.